

## Slab dehydration, intermediate-depth earthquakes, and arc magmatism: A review of seismological observations

NAKAJIMA, Junichi<sup>1\*</sup>

<sup>1</sup>RCPEV, Graduate School of Sci., Tohoku Univ.

We review recent seismological observations beneath the Japanese Islands and show important roles of geofluids on seismogenesis at intermediate depths and arc magmatism.

Seismicity in the subducting crust of cold slabs is most active at depths of 70-90 km, where seismic velocity in the crust abruptly increases, suggesting that high pore pressures generated as a result of dehydration reactions in the crust facilitate intermediate-depth seismicity. In contrast, seismicity is almost absent in the subducting crust of warm slabs like Cascadia and Nankai. The aseismic crust may be explained by slow dehydration rates in warm slabs, which cannot increase pore pressures effectively.

Magmatism beneath the arc has been discussed in terms of the heterogeneities in seismic velocities together with geochemical and petrological constraints. We recently developed simple but useful method to estimate seismic attenuation structures and applied it to waveform data in NE Japan. Seismic attenuation provides additional insights into ongoing magmatic processes in subduction zones, because higher-temperature environments or the existence of fluids may have different effects on seismic attenuation from on seismic velocity. The obtained results show that a depth profile of  $Q_p^{-1}$  in the back-arc mantle is explained by attenuation expected for a two-dimensional (2-D) thermal model. However, an inclined high-attenuation zone observed in the back-arc mantle wedge, which is interpreted as an upwelling flow, shows higher attenuation than that calculated from the 2-D thermal model. The higher seismic attenuation is probably caused by the concentration of partial melt in the upwelling flow. Our results further imply the breakdown of hydrous minerals in a hydrous layer above the Pacific plate at a depth of ~120 km.

Keywords: dehydration, pore pressure, eclogitization, seismic attenuation

## Imaging mantle melting processes and the effect of water beneath island arcs and backarc spreading centers

WIENS, Douglas<sup>1\*</sup> ; WEI, S. shawn<sup>1</sup>

<sup>1</sup>Washington University, St Louis, MO, USA

We use arrays of land and ocean bottom seismographs to image melting processes in the Mariana and Tonga-Lau mantle wedges. Both regions show arc volcanism, active backarc spreading, and a gradient in mantle water content going from slab to backarc spreading center. The Lau backarc in particular shows a gradient in inferred mantle water content as the spreading centers approach the arc and slab in the south. Water contents range from near-MORB conditions in the Central Lau Spreading Center (CLSC) to high water content for the Eastern Lau Spreading Center (ELSC) and nearly arc-like for the Valu Fa Ridge (VFR).

For both Mariana and Lau we find significant slow velocity and high attenuation anomalies in the upper 100 km of the mantle beneath the volcanic arc and the spreading center. In the Mariana region, the anomalies are separated by a high velocity, low attenuation region at shallow depths (<80 km), implying distinct arc and backarc melting regions, with the anomalies coalescing and possibly allowing material interchange at greater depths. The maximum anomaly in the backarc is shallower (~30 km) than in the arc (~65 km), consistent with geochemical indications on the depth of melt production in these regions. The strongest anomaly beneath the backarc spreading center is narrow (~70 km) and extends from close to the moho to 80 km depth. Data analyses for the Tonga-Lau project are preliminary, but show similarities to the Mariana images. Extremely low seismic velocity and high attenuation are found in a 100 km wide region beneath the spreading center in the upper 80 km. At deeper depths the anomaly is displaced westward in both velocity and attenuation images, suggesting that partial melting occurs along an upwelling limb of mantle flow originating west of the backarc. 3-D images from Rayleigh wave tomography show a much stronger anomaly along the CLSC when compared to the southern ELSC and VFR. The backarc velocity and attenuation anomalies are stronger in the Lau basin than in the Mariana backarc, perhaps due to higher mantle temperatures inferred from petrology.

Both Q and velocity anomalies are larger than expected for temperature effects based on laboratory-derived relationships, and their configuration is inconsistent with the expected temperature field. In addition, the observed anomalies are roughly inversely proportional to inferred mantle water content, suggesting that water content does not cause the observed large seismic anomalies. However, experimental results suggest that seismic attenuation and velocity are highly sensitive to the presence of even very small amounts of partial melt. Therefore we suggest the high attenuation and low velocity anomalies delineate the melt production regions beneath the ridge axis and volcanic arc, but that only small melt fractions (<1 %) are required to explain the seismic data. Smaller amplitude anomalies beneath the VFR, where large amounts of subduction-derived water are incorporated into the melt, may indicate lower mantle melt porosity due to low melt viscosity and more efficient transport of the water-rich melt, or a different topology of melt in the matrix. A lower melt porosity for aqueous melts is also consistent with the smaller seismic anomaly seen for the water-rich volcanic arc melting regions compared to the backarc melt production zone for both regions.

Keywords: seismic tomography, island arcs, backarc spreading centers, seismic attenuation, mantle fluids, melt generation

## Slab Melting in Subduction Zones

SCHMIDT, Max<sup>1\*</sup> ; MANN, Ute<sup>1</sup>

<sup>1</sup>ETH Zurich, Switzerland

Depending on temperature, slab-to-mantle element transfer in the subarc region may either occur through fluids or melts. In this contribution we present pelite melting experiments systematically varying H<sub>2</sub>O and CO<sub>2</sub> contents and review the presently available information on slab melting. Synthetic pelite model compositions containing variable proportions of H<sub>2</sub>O (0.7-4.4 wt%) and CO<sub>2</sub> (0-4 wt%) was melted at 3-4.5 GPa and 750-1200 °C. The fluid-saturation concentration at 3-8 GPa (i.e. the H<sub>2</sub>O stored in phengite as the only hydrous phase) is 0.8-0.9 wt% H<sub>2</sub>O. We locate the fluid-absent solidus of the H<sub>2</sub>O-pelite system at 3 to 4.5 GPa at 880 °C to 1050 °C about 150-200 °C higher than the wet solidus (3 to 4.5 GPa, 730 to 860 °C). CO<sub>2</sub> increases the fluid-saturated solidus temperature by ~30 °C but leaves the fluid-absent solidus temperature unchanged. For all systems considered, the onset of melting is controlled by phengite and only in the fluid-absent experiments K-feldspar becomes a product of melting (at 3 GPa).

Compiling all available information, we parameterize the amount of melt to be formed as a function of temperature for fluid-saturated and fluid-undersaturated conditions. Melt compositions themselves are meta- to peraluminous high Si-granites (71-77 wt% SiO<sub>2</sub> on a volatile free basis) with low Fe, Mg, and Ca contents and are uniform to ~50% melting when plotted as a function of melt fraction (but not temperature), almost independent of starting compositions. At >2 wt% bulk H<sub>2</sub>O melts are sodic (K/Na=0.2-0.4), while at <1.5 wt% melts are mostly potassic (K/Na=0.9-1.7). Only the fluid-poor H<sub>2</sub>O-CO<sub>2</sub> and the CO<sub>2</sub>-only experiments of Thomsen and Schmidt (2008, EPSL) and Tsuno and Dasgupta (2011, CMP) produce significantly different melts i.e. rather potassic phonolites (Na being increasingly retained in jadeitic cpx with pressure). Near 5 GPa a fundamental change occurs: the H<sub>2</sub>O-silicate solidus comes to an endpoint while in CO<sub>2</sub>-rich systems a carbonatite replaces the silicate melt lowering the solidus temperature by more than 100 °C to 9 GPa.

Regarding the likelihood of sediment melting in the subarc region, only the wet solidus is within reach of the hottest geotherms of the thermal models that predict the highest slab-surface temperatures, i.e. none of the Arcay et al (2007, EPSL) slab surface P-T paths cross the solidus while for Syracuse et al. (2010, G3) about 7 out of 56 modeled slab segments have P-T-paths that may lead to significant melting for H<sub>2</sub>O-saturated pelites at 3-4 GPa. As retention of significant amounts of fluids within a subducting lithology is not an option, flushing with fluids from dehydrating serpentinites would be the only option for achieving significant melting in the hottest subduction zones (at the required P-T conditions, there are no suitable reactions in the mafic crust or the sediments themselves). An alternative option to reach widespread pelite melting would be to dismiss the rigid slab surface concept and allow for sediment diapirs to rise into the hot mantle (Gerya and Yuen, 2003, EPSL; Behn et al, 2011, Nature Geosci.) in which case the pelites could bleed out their incompatible elements completely. Nevertheless, these diapirs are propelled by a density contrast resulting from partial melting and it remains unclear whether they could start rising without melting in the first place.

In conclusion, combining P-T paths, phase diagrams and degrees of melting suggests that significant pelite melting at a rigid slab-mantle interface appears to be a rather rare on present day Earth (and hence much more so for mafic materials), the only option for widespread pelite melting appears to be entrainment of the sediments into the mantle wedge. Removal of CO<sub>2</sub> through melting is utterly inefficient and as subsolidus metamorphic reactions lead to low X<sub>CO2</sub> fluids, most of the subducted CO<sub>2</sub> will be fed into the deep beyond-arc C-cycle.

Keywords: slab melting, H<sub>2</sub>O, CO<sub>2</sub>, pelite

## Diverse magmatic effects of subducting a hot slab in SW Japan: results from forward modeling

KIMURA, Jun-ichi<sup>1\*</sup> ; GILL, James<sup>2</sup>

<sup>1</sup>JAMSTEC, <sup>2</sup>University of California Santa Cruz

In response to the subduction of the young Shikoku Basin of the Philippine Sea Plate, arc magmas erupted in SW Japan throughout the late Cenozoic. Many magma types are present including ocean island basalt (OIB), shoshonite (SHO), arc-type alkali basalt (AB), typical sub-alkalic arc basalt (SAB), high-Mg andesite (HMA), and adakite (ADK). OIB erupted since the Japan Sea back-arc basin opened, whereas subsequent arc magmas accompanied subduction of the Shikoku Basin. However, there the origin of the magmas in relation to hot subduction is debated. Using new major and trace element and Sr-Nd-Pb-Hf isotope analyses of 324 lava samples from seven Quaternary volcanoes, we investigated the genetic conditions of the magma suites using a geochemical mass balance model, Arc Basalt Simulator version 4 (ABS4), that uses these data to solve for the parameters such as pressure/temperature of slab dehydration/melting and slab flux fraction, pressure, and temperature of mantle melting. The calculations suggest that those magmas originated from slab melts that induced flux-melting of mantle peridotite. The suites differ mostly in the mass fraction of slab melt flux, increasing from SHO through AB, SAB, HMA, to ADK. The pressure and temperature of mantle melting decreases in the same order. The suites differ secondarily in the ratio of altered oceanic crust to sediment in the source of the slab melt. The atypical suites associated with hot subduction result from unusually large mass fractions of slab melt and unusually cool mantle temperatures.

Keywords: SW Japan, Volcanic rocks, Geochemistry, Forward model

## Fluids and earthquakes in the Japan subduction zone

ZHAO, Dapeng<sup>1\*</sup>

<sup>1</sup>Tohoku University, Department of Geophysics

Detailed tomographic images are determined for the source areas of large crustal and megathrust earthquakes that occurred in the Japan subduction zone during 1995-2013, thanks to the availability of the dense Japanese seismic network that could locate accurately the mainshocks and aftershocks of those large earthquakes and provide high-quality arrival-time data for tomographic imaging. Suboceanic events are relocated precisely using sP depth phase. Large crustal earthquakes in the forearc region such as the 1995 Kobe earthquake (M 7.2) and the 2011 Iwaki earthquake (M 7.0) might be triggered by fluids that are released from the dehydration of the subducting slab and directly ascend to the crust and enter an active fault zone. In contrast, along the volcanic front and in back-arc areas, the seismogenic layer in the upper crust is thinned and its mechanical strength is weakened because of ascending hot magmas and fluids which are produced by a combination of slab dehydration and corner flow in the mantle wedge. Large crustal earthquakes are apt to take place at the edge portion of the thinned seismogenic layer which exhibits low velocity, high Poisson's ratio, and high electrical conductivity. To clarify the generating mechanism of the 2011 Tohoku-oki earthquake (Mw 9.0) and the induced tsunami, we determined high-resolution tomographic images of the Northeast Japan forearc. Significant lateral variations of seismic velocity are visible in the megathrust zone, and most large interplate thrust earthquakes are found to occur in high-velocity (high-V) areas. These high-V zones may represent high-strength asperities at the plate interface where the subducting Pacific plate and the overriding Okhotsk plate are coupled strongly. A shallow high-V zone with large coseismic slip near the Japan Trench may account for the mainshock asperity of the 2011 Tohoku-oki earthquake. Because it is an isolated asperity surrounded by low-velocity patches, most stress on it was released in a short time and the plate interface became decoupled after the Mw 9.0 earthquake. Thus the overriding Okhotsk plate there was shot out toward the Japan Trench and caused the huge tsunami. Further details of the role of arc magma and fluids in the nucleation process of a large earthquake can be clarified by high-resolution geophysical imaging and multidisciplinary studies of the earthquake fault zones.

Keywords: fluids, earthquakes, Japan Islands, subduction zones, magma, slab

## Silicate solute in aqueous fluids governs trace element and stable isotope behavior in subduction zones

MYSEN, Bjorn<sup>1\*</sup>

<sup>1</sup>Geophysical Laboratory, CIW, USA

Physical and chemical properties of fluids equilibrated with subducting deep crust and overlying upper mantle are saturated in silicate components [1]. These components govern physical and chemical properties of the fluids. For example, the solution behavior of volatile components such as hydrogen, carbon, and nitrogen, which form bonding with silicate components in fluids, will differ from the behavior in pure H<sub>2</sub>O fluids [2]. This can also affect isotope fractionation between fluids and condensed silicate materials.

In pure H<sub>2</sub>O, hydrogen bonding plays a role to temperatures <600 °C at pressures in the 1 GPa-range with a  $\Delta H$  for hydrogen bond formation near 20 kJ/mol. At temperatures less than 600 °C, physical properties of fluids, including density, compressibility, and viscosity, are non-linear functions of temperature, whereas at higher temperature and in the absence of hydrogen bonding, these properties tend to become linear functions of temperature. Solution of silicate components in aqueous fluids changes these relationship. The silica solubility in equilibrium with quartz/coesite reaches >5 mol/kg near 5 GPa and 900 °C with polymerized silicate species, SiO<sub>4</sub>, Si<sub>2</sub>O<sub>7</sub>, and SiO<sub>3</sub> in the fluid. In equilibrium with enstatite and forsterite, the silicate solubility is ~50% less and only SiO<sub>4</sub> and Si<sub>2</sub>O<sub>7</sub> species exist in the fluids. Those variables affect D/H isotope ratios. For example, the fluid/melt partition coefficients for hydrogen, KH, varies by ~40% as a function of variable silicate speciation in fluids in the 500 °C-800 °C/0.5-1 GPa temperature and pressure range. The hydrogen fluid/melt partition coefficient exceeds that of deuterium. Their temperature-dependence also differs so that for the exchange equilibrium of D and H between coexisting water-saturated melt and silicate-saturated aqueous fluid, the  $\Delta H$  is between -4 and -6 kJ/mol. This difference is because in the more silicate-rich fluids (higher proportion of polymerized silicate species), the abundance ratio, OD/OH, is higher in the more polymerized silicate species in the fluid. As a result, increasing pressure, which leads to increasingly polymerization of silicate, will cause the D/H ratio of the fluid will increase. This also means that D/H fractionation between aqueous fluid and condensed silicate increases with increasing pressure.

Interaction between dissolved silicate components and other elements can also affect their solubility and, therefore, their roles as geochemical tracers. For example, in the system rutile+H<sub>2</sub>O, the Ti solubility in the few-GPa-range at ~1000 °C is on the order of 1-100 ppm as compared with thousands of ppm in silicate-saturated aqueous solution [3]. This difference between pure H<sub>2</sub>O and silicate-saturated fluid is related to interaction with the silicate species dissolved in the fluid,  $2M_6Si_2O_7 + 4H_2O + TiO_2 = 4(MH)_2SiO_4 + M_4TiO_4$ , where M is a metal cation. Similar situation likely exist for other nominally insoluble, highly charged elements (e.g., Al<sup>3+</sup>, Zr<sup>4+</sup>, Hf<sup>4+</sup>, P<sup>5+</sup>).

When modeling isotope fractionation and partitioning of nominally insoluble elements between fluid and condensed phases (melts and minerals) in the deep crust and upper mantle of the Earth, the silicate solute concentration and structure in the fluid and the water concentration and structure of silicate melts both can have major effects on the fractionation factors. These factors depend on the element or isotope ratio in question. They also vary with pressure (and likely temperature) because the structure of dissolved silicate in aqueous fluids varies with pressure and temperature.

[1] C. E. Manning, *Eart Planet. Sci. Lett.* 2004, 223, 1-16.

[2] B. O. Mysen, *Lithos* 2012, 148, 228-246.

[3] A. Antignano and C. E. Manning, *Chemical Geology* 2008, 255, 283-293.

Keywords: aqueous fluid, solubility, subduction, stable isotope, structure, fluid property

## D/H intramolecular partitioning in alkali silicate melts: with implications for tracing subduction processes

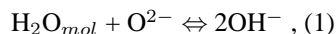
LE LOSQ, Charles<sup>1\*</sup> ; CODY, George<sup>1</sup> ; MYSEN, Bjorn<sup>1</sup>

<sup>1</sup>Geophysical Laboratory, Carnegie Institution of Washington

The D/H ratio is an important probe for studying the cycle of water in the Earth interior in general, and in subduction zones in particular. Indeed, D/H ratios in melt inclusions (MIs) of arc magmas for instance indicate that the  $\delta D$  of subduction fluids is high, near -30 ‰, compared to the  $\delta D$  of the mantle that is near -80 ‰. A possible explanation for these different values is that D/H fractionation during dehydration of the slab in subduction zones enriches the subduction fluids in D, leading to high  $\delta D$  values in subduction magmas. This might be accomplished with hydrogen exchange between the melt and another source enriched in D before entrapment of MIs or a diffusive loss of H from within the inclusion leading to D/H fractionation. However, chemical effects affecting the  $\delta D$  ratio have not been considered because it is usually assumed that D and H have the same chemical and structural properties in silicate melts and glasses.

However, recent results from <sup>2</sup>H and <sup>1</sup>H MAS NMR of Na<sub>2</sub>Si<sub>4</sub>O<sub>9</sub> glasses quenched from melt (equilibrated with fluid at 1400°C and 1.5 GPa) with various amounts of (D<sub>x</sub>H<sub>(1-x)</sub>)<sub>2</sub>O (x = D/[D+H]) lead to the conclusion that D and H isotopes occupy different structural positions in the network. From the <sup>1</sup>H MAS NMR spectra OH<sup>-</sup> groups are distributed in two environments with mean O...O distances close to 0.26 and 0.29 nm in the Na<sub>2</sub>Si<sub>4</sub>O<sub>9</sub> glass. These environments give rise to two strong NMR lines at 16 and 5 ppm respectively. By contrary, <sup>2</sup>H MAS NMR spectra of the same glasses display a strong line at 16 ppm accompanied by a small band near 5 ppm regardless of D/H ratio and total water concentration. This observation leads to the suggestion that OD<sup>-</sup> groups are mainly present in an environment with small O...O distances. In other words, the structural behavior of OH<sup>-</sup> and OD<sup>-</sup> groups in the quenched silicate melts (glasses) differs.

In M<sub>2</sub>Si<sub>4</sub>O<sub>9</sub> glasses, (M = Li, Na or K) with different concentrations of pure H<sub>2</sub>O or D<sub>2</sub>O (from 3.3 up to 17.6 mol%), <sup>2</sup>H and <sup>1</sup>H MAS NMR spectra confirm that by exchanging H with D the intensity of the 16 ppm NMR line increases greatly, whereas the intensity of the 5 ppm line decreases drastically. Interestingly, such a spectral evolution is also observed when increasing the size of the alkali element in the network of hydrous alkali silicate glass. These effects are attributed to steric and electronic effects in the environment of alkali elements, which cause shifts in the equilibrium between H<sub>2</sub>O and O<sup>2-</sup> of the silicate network:



The specific preference of OD<sup>-</sup> groups for small O...O sites is in this mind intriguing, but is not in conflict with previous observations. Indeed, increasing the ionic size of alkali elements lead to promote OH<sup>-</sup> in the small O...O environment. Similarly, it appears that increasing the size of the proton (by substituting H by D) promotes their existence in this small O...O environment. On this basis, we propose that those two observations have a common origin, maybe related to the probability of interaction between H/D and alkali elements depending of their ionic size and/or to molar volume effects related to those ionic sizes.

This large structural-controlled partitioning of D and H in melts, which depends on the melt composition, might be another fractionation process affecting the  $\delta D$  of subduction melts. Consequently,  $\delta D$  values recorded in MIs might be the result of such a structural process and might not reflect the  $\delta D$  of released fluids in the mantle wedge during slab subduction.

Keywords: D/H isotopes, silicate glass, NMR spectroscopy, Raman spectroscopy, Subduction fluids

## Speciation and solubility of F and Cl in coexisting fluids and silicate melts: implications for F and Cl signature in arc

DALOU, Celia<sup>1\*</sup> ; MYSEN, Bjorn<sup>2</sup> ; FOUSTOUKOS, Dionysis<sup>2</sup>

<sup>1</sup>Jackson School of Geosciences, The University of Texas at Austin, <sup>2</sup>Geophysical Laboratory, Carnegie Institution of Washington

The effect of pressure and temperature on the structure of silicate melts coexisting with silica-saturated aqueous electrolyte solutions enriched in fluorine or chlorine in the  $\text{Na}_2\text{O}-\text{Al}_2\text{O}_3-\text{SiO}_2-\text{H}_2\text{O}$  system has been determined. In-situ measurements were conducted with the samples at desired temperatures and pressures in a hydrothermal diamond anvil cell (HDAC) by using microRaman and FTIR spectroscopy techniques. The data were acquired at high temperature and pressure (up to 800°C and 1264 MPa, respectively), and during cooling/decompression to ambient conditions.

The intensity of the Raman bands assigned to stretch vibration of the OH-groups relative to those of coexisting molecular  $\text{H}_2\text{O}$  in silicate melts is lower in the presence of F and Cl. This difference reflects the interaction of F or Cl with  $\text{H}_2\text{O}$  in the melts. With decreasing pressure and temperature (P-T) conditions, SiF complexes are favored in the melt rather than in the fluid, perhaps because of decreasing silicate concentration in fluids with decreasing temperature and pressure. In melts, the solubility of Cl, likely in the form of  $\text{NaCl}_{(aq)}$ , increases with decreasing P-T conditions, whereas the abundance of such complexes in coexisting fluids decreases.

Our experiments data were employed to help model the ascent of a magma-fluid system from the upper mantle to the shallow crust. The information offers particular insights into F and Cl partitioning between and the speciation of F and Cl in melts and magmatic fluids. We suggest that the formation of stable SiF and NaCl complexes and their increasing solubilities during magma ascent explain the late volcanic degassing of F and Cl, compared to other volatile species.

It explains why F and Cl are often undersaturated in arc basaltic magmas (Carroll and Webster, 1994), indicating that they often do not a significant experience a degassing event. In contrast to  $\text{H}_2\text{O}$ ,  $\text{CO}_2$  and S, F and Cl signature in primary arc magmas (arc melt inclusions) can be considered as primary and likely retain information on arc magma sources.

Those results also imply that, while Cl is enriched in aqueous fluids from slab dehydration, F preferentially dissolves in slab melts or supercritical fluids, during flows from the subducted slab into the zone of melting in the mantle wedge. It is therefore expected that at given pressure and temperature, the Cl/F ratio is significantly lower in slab melt and supercritical fluids, than in aqueous fluids. This difference in Cl/F signatures decrease when slab components are dragged down to the deep mantle.

Keywords: Fluorine, Chlorine, silicate melt, aqueous fluid, speciation, HDAC

## The Structure of Water-Saturated Carbonate Melts

FOUSTOUKOS, Dionysis<sup>1\*</sup>; MYSEN, Bjorn O.<sup>1</sup>

<sup>1</sup>Geophysical Laboratory, Carnegie Institution of Washington, USA

The structure of water-saturated Ca- and Mg-bearing carbonate melts under reducing and oxidizing conditions was investigated in a series of hydrothermal anvil cell experiments conducted at 400 - 1100 °C and 442 - 2839 MPa. Equilibria were investigated in the calcite-H<sub>2</sub>O, calcite-CaO-H<sub>2</sub>O, magnesite-H<sub>2</sub>O and magnesite-MgO-H<sub>2</sub>O systems, with redox conditions controlled by Re/ReO<sub>2</sub> and Ti/TiO<sub>2</sub> assemblages. Melting relationships and the C-O-H speciation of the coexisting aqueous fluid and melt were assessed in-situ by Raman vibrational spectroscopy. Hydrous melting of MgCO<sub>3</sub>-MgO occurred at ~850 °C, 1.5 - 2 GPa. In the CaCO<sub>3</sub>-CaO-H<sub>2</sub>O system, melt was formed at 600 - 900 °C and pressures of 0.5 - 1.5 GPa because of melting-point depression imposed by the presence of CaO. The C-O-H speciation of the carbonate melts and coexisting supercritical aqueous solutions was mainly H<sub>2</sub>O and CO<sub>3</sub><sup>2-</sup>, with traces of CO<sub>2(aq)</sub> and CH<sub>4(aq)</sub> in the fluid phase. The melt-fluid H<sub>2</sub>O partition coefficients attained in the Mg-bearing melt (median 0.5) were higher than in the Ca-bearing melt (median 0.3). Under oxidizing redox conditions, dissolved ReO<sub>4</sub><sup>-</sup> was present in all phases, underscoring the enhanced solubility of trace elements and metals in carbonate-bearing melts and carbonatites. In effect, the enhanced solubility of H<sub>2</sub>O along with the ionic nature of the carbonate melts may promote the solvation of ionic species in the melt structure.

From in-situ vibrational spectroscopy, the ν<sub>1</sub>-CO<sub>3</sub><sup>2-</sup> vibration recorded in the melt spectra suggests the presence of intermolecular interactions between the oxygen of the carbonate ion with water dissolved in the melt. The thermodynamic properties of this water appear to be similar to the supercritical aqueous phase. For example, the estimated enthalpy for the breakage of the hydrogen bonding between water molecules attained values of 6.8 ± 1.5 kcal/mol and 8.4 ± 1.3 kcal/mol in the melt and fluid phase, respectively. The calculated partial molar volume of H<sub>2</sub>O in the melt (~48 ± 6 cm<sup>3</sup>/mol) is also comparable to the partial molar volume of supercritical water at similar conditions. Interestingly, this value is considerably greater than published partial molar volume values for H<sub>2</sub>O in silicate melts (10-12 cm<sup>3</sup>/mol).

The pressure-temperature melting relationships of the CaO-CO<sub>2</sub>-H<sub>2</sub>O and MgO-CO<sub>2</sub>-H<sub>2</sub>O systems highlight the important role of water and alkali earth oxides on the hydrous melting of the carbonate-bearing subducting oceanic crust. Carbonates present in marine sediments or serpentinized peridotites may melt before complete dehydration at the slab-mantle wedge transition zone, and thus, never reach sub-arc depths. To this end, melting of carbonate minerals at crustal temperatures and pressure can contribute to the volcanic CO<sub>2</sub> flux at the arc through melt/fluid interactions.

Keywords: carbonate melt, aqueous solutions, hydrothermal diamond anvil cell, raman vibrational spectroscopy

## Later phase observations and seismic velocity structure in the subducting crust of the Pacific slab beneath Hokkaido

SHIINA, Takahiro<sup>1\*</sup> ; NAKAJIMA, Junichi<sup>1</sup> ; TOYOKUNI, Genti<sup>1</sup> ; MATSUZAWA, Toru<sup>1</sup> ; KITA, Saeko<sup>2</sup>

<sup>1</sup>RCPEV, Grad. Sch. of Sci., Tohoku Univ., <sup>2</sup>NIED

The subducting crust at the uppermost part of the oceanic lithosphere is considered to play important roles for generation of intraslab earthquakes (e.g., Kirby et al., 1996) and arc-magmatism in the mantle wedge (e.g., Nakajima et al., 2013), because the crust involves a large amount of water in form of hydrous minerals and these hydrous minerals affect seismic velocities in the crust (e.g., Hacker et al., 2003). Therefore, to understand water circulation in the subduction zones and genesis of intermediate-depth earthquakes, it is important to reveal where dehydration reaction of hydrous minerals occurs in the crust. However, it is generally difficult to obtain the detailed velocity variation in the crust because the thickness of the crust is ~7 km.

Later phases, such as mode-converted wave and guided wave, are sensitive to heterogeneous structure in the crust because of their longer propagation paths in the crust, and hence they are very useful to resolve small-scale seismic velocity structure in the crust (e.g., Matsuzawa et al., 1986; Abers, 2005).

At the Hidaka mountain range, middle of Hokkaido, northern Japan, some later phases are reported from earthquakes that occurred in the Pacific slab (e.g., Shimizu and Maeda, 1980). A later phase (Xp phase) recorded in this region has some characteristics: 1) amplitudes of Xp phase are similar to or larger than those of the P wave, 2) Xp-P time lies in a range of 2-10 s and increases with epicentral distances. Shiina et al. (2013, SSJ) discussed the origin of the Xp phase with numerical modeling and interpreted the Xp phase as guided P-wave that propagated in the crust. Moreover, we identified a later phase (Xs phase) that arrives several second after the theoretical initial S waves, and such a phase usually appears in seismograms with guided P-wave. We interpreted the Xs phase as guided S-wave by comparison characteristics of guided P-wave and results of numerical modeling.

In this study, based on these interpretations for later phases that observed in the western part of Hidaka mountain range, we estimated P- and S-wave velocity distributions in the subducting crust beneath the eastern part of Hokkaido. The number of arrival times of guided P- and S-waves picked in this study is 117 records and 56 records, respectively. Then, we obtained Vp of 6.8-7.7 km/s and Vs of 3.5-4.0 km/s at depths of 50-100 km in the crust. The obtained Vp in the crust is similar to that observed beneath Tohoku (Shiina et al., 2013) and lower than that expected for fully-hydrated MORB materials (e.g., Hacker et al., 2003). This result suggests that aqueous fluids may co-exist with hydrous minerals in the crust beneath the eastern part of Hokkaido.

Keywords: subducting crust, later phase, guided wave, the Pacific slab

## Pore fluid geochemistry and carbonates in cores and cuttings from the Nankai accretionary prism

EVEN, Emilie<sup>1\*</sup> ; SAMPLE, James C.<sup>2</sup> ; FUCHIDA, Shigeshi<sup>1</sup> ; IODP EXPEDITION 348, Shipboard scientists<sup>3</sup>

<sup>1</sup>Graduate School of Science, Osaka City University, <sup>2</sup>School of Earth Sciences and Environmental Sustainability, Northern Arizona University, <sup>3</sup>IODP Expedition 348

The recent IODP Exp 348 at Site C0002 has successfully deepened Hole C0002F (Exp 338) down to 3058.5 mbsf, deep into the accretionary prism of the Nankai Trough. During Exp 348, cuttings were collected and analysed from drilled interval of Holes C0002N (875 mbsf- 2325 mbsf) and C0002P (1965 mbsf- 3059 bsf) and limited coring was performed from 2163 to 2218 mbsf in Hole C0002P. The major-element composition of the solid cuttings and the geochemistry of interstitial water in cores was determined. Results provide insights into exchange of elements between minerals and pore water phases, and into geochemical signatures related to lithological changes within the prism. This study reports the main geochemical results from IODP Exp 348.

Interstitial waters were collected using the GRIND method (Wheat et al., 1994), in which core sediments were ground in an agate mill with ultra-pure water. The interstitial water percentage was determined by drying sediments at 60 °C and 105 °C, the former to minimize loss of clay-bound water, and the latter to follow the GRIND procedure used in previous expeditions. Concentrations were interpreted with data corrected for dilution at 60 °C, 105 °C and normalised to chlorinity values. Profiles of carbonates (as CaCO<sub>3</sub>), organic carbon and total nitrogen were determined from cuttings of 1-4 mm and >4 mm sizes and are compared with the observed lithological boundaries. Carbonate veins were observed in a core sample exhibiting a fault zone at ~2205 mbsf, but no increase was observed at the same depth in the carbonates profile.

The GRIND method has limitations in recovering absolute values of dissolved ions in interstitial waters, and yielded very high dissolved-ion concentrations in some samples. But comparison of ions normalized to chlorinity yielded results comparable to what was observed in pore waters at shallower depths of Site C0002. Some of the trend variations in the cuttings profiles of carbonates, organic carbon and nitrogen match the unit boundaries determined by observation of lithological changes in the cuttings. Therefore, it can be suggested to integrate these data when defining geological units.

*Wheat, Boulegue and Mottl (1994) Proc. ODP, Sci. Results, 139: College Station, TX (Ocean Drilling Program), 429-437*

Keywords: Accretionary prism, GRIND method, IODP Expedition 348, Nankai Trough, Pore water

## Solution mechanism of water in depolymerized silicate melts

CHERTKOVA, Nadezda<sup>1\*</sup> ; YAMASHITA, Shigeru<sup>1</sup>

<sup>1</sup>Okayama University, ISEI

It is known that the effect of dissolved water on the viscosity of silicate melts is larger for polymerized melts than for depolymerized melts [e.g., 1, 2]. Direct spectroscopic measurements of melt structure and water speciation at high temperature provide information about the mechanism of water dissolution and its influence on the physical properties of the melts. While *in situ* measurements of water speciation were widely conducted for rhyolitic melts and their analogues [e.g., 3, 4, 5], only limited data are available for depolymerized silicate melts.

We performed high-temperature near-infrared and Raman spectroscopic measurements of hydrous  $\text{Na}_2\text{Si}_2\text{O}_5$  melts (2.3-8.1wt%  $\text{H}_2\text{O}$ ) using externally heated diamond anvil cell (HDAC).  $\text{Na}_2\text{Si}_2\text{O}_5$  composition was chosen as a structural analogue of basaltic melt (anhydrous NBO/T = 1). Experimental pressure was monitored with the pressure- and temperature-dependent Raman shift of  $^{13}\text{C}$  diamond [6]. Near-infrared spectra of the homogeneous liquid phase, observed above 820 degree C, 1.7GPa in the  $\text{Na}_2\text{Si}_2\text{O}_5+2.3\text{wt}\%\text{H}_2\text{O}$  system and above 700 degree C, 1.6GPa in the  $\text{Na}_2\text{Si}_2\text{O}_5+8.1\text{wt}\%\text{H}_2\text{O}$  system, contain absorption peaks corresponding to molecular  $\text{H}_2\text{O}$  (at  $\sim 5200\text{ cm}^{-1}$ ) and structurally bound OH groups (at  $\sim 4500\text{ cm}^{-1}$ ). At 900 degree C and 1.6-1.9GPa the ratio of these peaks height remains approximately constant (2.6-2.2), implying a constant (structurally bound OH)/(molecular  $\text{H}_2\text{O}$ ) ratio for this range of water contents. This observation differs from the regularities reported for more polymerized melts (rapid decrease of OH/ $\text{H}_2\text{O}$  with total water content) [e.g., 4, 7]. At the same time no pressure effect on the ratio of  $4500\text{ cm}^{-1}$  peak height to  $5200\text{ cm}^{-1}$  peak was observed below 2.4 GPa.

### References

- [1] Whittington A., Richet P., Holtz F. (2000) *Geochim Cosmochim Acta* 64, 3725-3736.
- [2] Giordano D., Russell J.K., Dingwell D.B. (2008) *Earth. Planet. Sci. Lett.* 271, 123-134.
- [3] Sowerby J.R., Keppler H. (1999) *Am. Mineral.* 84, 1843-1849.
- [4] Nowak M., Behrens H. (2001) *Earth. Planet. Sci. Lett.* 184, 515-522.
- [5] Shen A.H., Keppler H. (1995) *Am. Mineral.* 80, 1335-1338.
- [6] Mysen B.O., Yamashita S. (2010) *Geochim. Cosmochim. Acta* 74, 4577-4588.
- [6] Mysen B.O. (2010) *Geochim. Cosmochim. Acta* 74, 4123-4139.
- [7] Botcharnikov R.E., Behrens H., Holtz F. (2006) *Chem. Geol.* 229, 125-143.

Keywords: water speciation, hydrothermal diamond anvil cell, near-infrared spectroscopy, Raman spectroscopy